Organic LETTERS

Letter

pubs.acs.org/OrgLett

Organocascade Synthesis of Annulated (*Z*)-2-Methylenepyrans: Nucleophilic Conjugate Addition of Hydroxycoumarins and Pyranone to Branched Nitro Enynes via Allene Formation/Oxa-Michael Cyclization/Alkene Isomerization Sequence

Ramani Gurubrahamam, Bing-Fong Gao, Yan ming Chen, Yu-Te Chan, Ming-Kang Tsai,* and Kwunmin Chen*

Department of Chemistry, National Taiwan Normal University, Taipei 11677, Taiwan R.O.C

Supporting Information

ABSTRACT: An efficient organocatalytic reaction using 1,3-nitro enynes with 4-hydroxycoumarin and 4-hydroxy-6-methyl-2-pyrone to afford pyrano-annulated scaffolds in high yield (up to 88% yield) and excellent stereoselectivities (up to >20:1 dr and >99% ee) is described. The reaction proceeded through sequential conjugate addition, allene formation, intramolecular oxa-Michael 6-*endo*-*dig* cyclization and DABCO-catalyzed olefin isomerization. A kinetic profile for isomerization was established. The mechanism for the organocascade reaction was proposed according to requisite computational and mechanistic experimental studies.

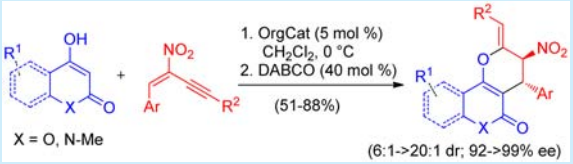

Enynes are useful building blocks for a variety of synthetic transformations to generate complex structural skeletons.[1] Stereoselective reactions on linear nitro enynes were developed by combining organo- and metal catalysis in the presence of various nucleophiles.[2] Alexakis and co-workers successfully employed sequential chiral enamine and gold catalysis for asymmetric conjugate addition of aldehydes to monosubstituted nitroolefin followed by electrophilic activation of the triple bond (Scheme 1a).[2a,b] The same strategy was used for conjugate addition of malonates/oxindoles to nitro enynes by Shao[2c] and Zhou et al.[2d] Recently, Enders et al. developed various asymmetric protocols by merging organocatalysis with silver catalysis to afford pyranoannulated pyrazoles,[3a] naphthoquinones,[3b] coumarins,[3c] and spiropyrazolones[3d] by using linear 1,3-nitro enynes, enynones, and 1,5-nitro enynes (Scheme 1b).[4] Lewis acidic metal was used to activate the alkyne group for further transformation.

Scheme 1. Strategies for Reaction on Activated 1,3-Enynes

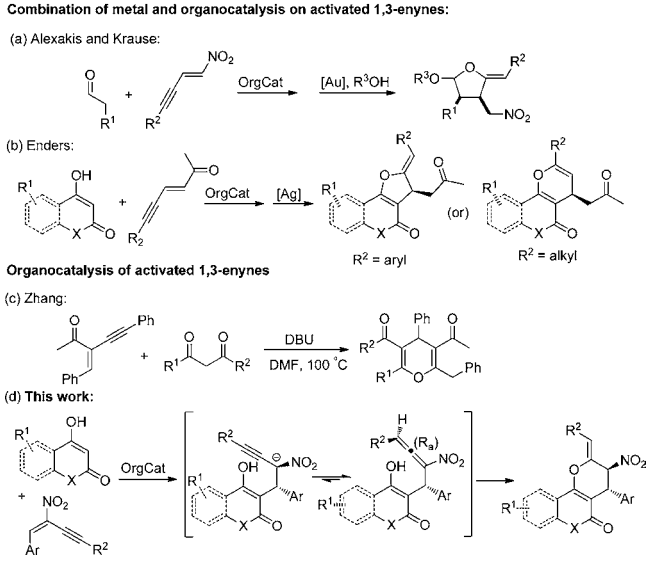

Numerous strategies for chiral allene synthesis from alkynes and conjugated enynes were reported aside from sporadic examples of asymmetric organocatalytic methods.[5] The resulting 1,3-allene is a useful moiety for further site-, chemo-, and/or stereoselective functionalization through axial-to-central chirality transformation.[6] Melchiorre et al. merged the in situ allene formation and cyclization reaction under organo- and silver metal catalysis from branched enynone precursors to form functionalized furans.[7] On the other hand, Zhang's group developed an organocatalytic protocol to afford annulated products by using branched activated enynes (Scheme 1c).[8] However, the catalytic asymmetric variant remains a daunting challenge.[9] In continuation of our organocascade reactions on α,β-disubstituted nitroolefins,[10] we envisioned that α-alkynyl-branched nitroolefins[11] would be appropriate Michael acceptors and the resultant electron-rich nitro propargylic carbon anion would render susceptible isomerization to nitroallene.[12] We anticipated that further functionalization might occur in the in situ generated nitroallenes with an enol as a nucleophilic site (Scheme 1d).

To implement this hypothesis, we attempted the conjugate addition of 4-hydroxycoumarin **1a** across the nitroolefin

Received: April 30, 2016
Published: June 21, 2016

DOI: 10.1021/acs.orglett.6b01265
Org. Lett. 2016, 18, 3098−3101

component of the branched 1,3-enyne **2a** under bifunctional squaramide **I** catalysis. We observed cascade *anti-Z*-**3a**, *anti-E*-**3a**, and isomerized (**4a**) products in 77% overall yield (*Z*)-**3a**/**4a**/(*E*)-**3a** = 2:1:4), and the enantioselectivity of the (*E*)-**3a** was determined to be 95% ee (Table 1, entry 1). Neither the conjugate addition product nor the resulting nitroallene was observed under these reaction conditions.

Table 1. Optimization for the Cascade Reaction[a]

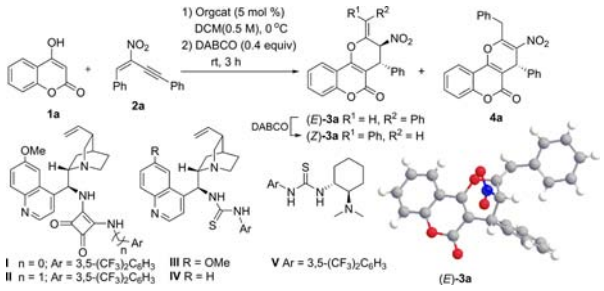

entry	cat.	time (h)	(*Z*)-**3a**/**4a**/(*E*)-**3a**[b]	yield[c] (%)	% ee[d,e]
1[f]	**I**	5	2:1:4	77	95[g]
2	**I**	5	19:1:—	65	95
3	**II**	4	>20:1:—	56	85
4	**III**	1.5	>20:1:—	62	89
5	**IV**	2.5	>20:1:—	55	61
6	**V**	2.5	17:1:—	55	−91
7[h]	**I**	5	14:1:—	74	95

[a]The reactions were carried out with **1a** (0.22 mmol) and **2a** (0.2 mmol) using organocatalyst (5 mol %) at 0 °C in DCM. [b]Determined by ^{1}H NMR crude analysis. [c]Isolated yield. [d]Determined from chiral HPLC analysis. [e]ee for (*Z*)-**3a** unless mentioned. [f]Without DABCO additive. [g]ee for (*E*)-**3a**. [h]DABCO addition at 0 °C.

Encouraged by this preliminary observation, we moved our focus to transforming all three isomers to a plausible single isomerized product **4a** under additional base catalysis. To our satisfaction, (*E*)-**3a** was completely converted into (*Z*)-**3a** as a major product after DABCO (0.4 equiv) treatment.[13] The (*Z*)-**3a** was isolated in 65% yield, and the enantioselectivity was retained in the diastereoconvergent process (*Z*)-**3a**:**4a** = 19:1, 95% ee) (Table 1, entry 2). Out of the other examined bifunctional catalysts (**II**−**V**), Takemoto's catalyst **V** afforded the antipodal isomer (*ent-Z*-**3a**) in moderate yield (55% yield, (*Z*)-**3a**:**4a** = 17:1) with good enantioselectivity (91% ee) (Table 1, entry 6). Furthermore, we attempted to optimize the reaction with different solvents, catalyst loadings, and temperatures by using chiral squaramide catalyst **I**. The reaction was not completed even after 6 days at low temperature (−10 °C) in DCM, and comparable enantioselectivity was observed at low catalyst loading (1−2 mol %), but only after prolonged reaction times (36−48 h).[13] Further, improvement in chemical yield of (*Z*)-**3a** was observed when isomerization process was carried out at 0 °C (Table 1, entry 7).

The reaction was generalized by selecting substituted 4-hydroxycoumarins (**1b**,**c**) and 4-hydroxy-6-methyl-2-pyrone **1e** as nucleophiles with various 1,3-enynes (**2b**−**f**) containing different aryl groups at nitroolefin and alkyne components by using the optimized conditions (Table 2). The enantioselectivity of the organocascade products with 4-hydroxycoumarin **1a** was maintained, irrespective of the substituent change either at nitroolefin or at the alkyne component of the 1,3-enyne. However, comparable yields and isomeric selectivity were

Table 2. Substrate Scope[a]

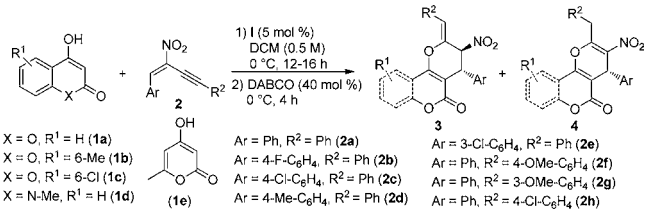

entry	1	2	(*Z*)-**3**:**4**[b]	yield[c] (%)	% ee[d,e]
1	**1a**	**2b**	8:1	79	95 (**3b**)
2	**1a**	**2c**	15:1	65	95 (**3c**)
3	**1a**	**2d**	12:1	88	95 (**3d**)
4	**1a**	**2f**	>20:1	81	95 (**3e**)
5	**1a**	**2g**	12:1	77	95 (**3f**)
6	**1b**	**2a**	10:1	74	>99 (**3g**)
7	**1c**	**2a**	14:1	71	92 (**3h**)
8[f]	**1d**	**2a**	5:1	52	95 (**3i**)
9	**1e**	**2a**	11:1	80	98 (**3j**)
10	**1e**	**2b**	8:1	81	98 (**3k**)
11	**1e**	**2c**	9:1	61	98 (**3l**)
12	**1e**	**2d**	16:1	87	98 **3m**)
13[f]	**1e**	**2e**	6:1	58	97 (**3n**)
14	**1e**	**2h**	15:1	59	99 (**3o**)
15[g]	**1e**	**2a**	11:1	52	98 (**3j**)

[a]The reactions were carried out with **1** (0.22 mmol) and **2** (0.2 mmol) using organocatalyst **I** (5 mol %) at 0 °C in DCM (0.5 M). [b]Determined by ^{1}H NMR crude analysis. [c]Isolated yield. [d]Determined from chiral HPLC analysis. [e]ee for (*Z*)-**3**. [f]2 days. [g]Reaction was carried out with 1.0 mmol scale.

observed for all of the products (**3b**−**f**) containing electron-releasing and -withdrawing groups (Table 2, entries 1−5). The 4-hydroxy-6-methylcoumarin **1b** with 1,3-enyne (**2a**) afforded the product in good yield with higher enantioselectivity (**3g**, 74% yield, >99% ee) than that of 6-chloro-4-hydroxycoumarin **1c** (**3h**, 71% yield, 92% ee) (Table 2, entries 6 and 7). The pyrano-annulated coumarin skeletons are crucial scaffolds because these are ubiquitous in numerous natural products and biologically active motifs.[14] We also used 4-hydroxy-1-methyl-1,2-dihydroquinolin-2-one **1d** as a nucleophile in the cascade reaction. The reaction was found to be slow, and after a prolonged reaction time (2 days), the corresponding pyranoannulated quinolinone **3i** was obtained in moderate yield (52%) with high enantioselectivity (95% ee) (Table 2, entry 8).

Next, we explore the organocascade process by using the analogous nucleophile 4-hydroxy-6-methyl-2-pyrone (**1e**) to obtain pyranopyrones (**3j**−**o**). The pyranoannulated pyranones are important skeletons because they possess diverse biological activities.[15] The 4-hydroxy-6-methyl-2-pyrone (**1e**) nucleophile afforded the corresponding products (**3j**−**o**) in good yields (up to 87% yield) with excellent stereoselectivity (97 to >99% ee) regardless of the electronic characteristics of the 1,3-enynes (**2a**−**h**) (Table 2, entries 9−14). To show the practical utility of our organocascade process, we attempted large-scale synthesis of the pyranoannulated pyrone **3j**. We obtained the product in good yield and sustainable enantioselectivity (98% ee) (Table 2, entry 15). The relative configuration of (*E*)-**3a** was unambiguously established from its single-crystal X-ray structural analysis (Table 1).[16] The stereogenic center of an aryl group in the pyranoannulated product (*E*)-**3a** was tentatively assigned from Michael addition of 4-hydroxycou-

DOI: 10.1021/acs.orglett.6b01265
Org. Lett. 2016, 18, 3098−3101

marin to nitroolefins under quinine derived squaramide bifunctional catalysis.[17] The configuration of the (*Z*)-**3a** was tentatively assigned from that of its educt (*E*)-**3a**.

We performed a few controlled experiments to gain more mechanistic insights into this organocascade reaction. We subjected (*E*)-**3a** (93% ee) to DABCO-catalyzed conditions to identify any discrepancy in enantioselectivity before and after the isomerization process. We isolated the desired product (*Z*)-**3a** in 89% yield without any erosion in enantioselectivity (Scheme 2a). We also subjected the (*Z*)-**3a** isomer to possible

Scheme 2. Controlled Experiments

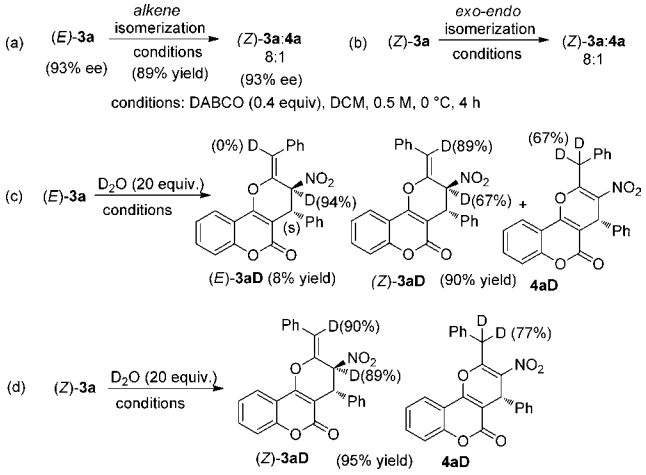

exo−*endo* isomerization under basic conditions and found that it led to a mixture of (*Z*)-**3a** and **4a** (8:1) under our optimized conditions (Scheme 2b). Next, we conducted an isomerization process in the presence of deuterium oxide to investigate the deuterium incorporation. The diastereoconvergent process yielded a (*Z*)-**3aD** product containing deuterium at $-NO_2$ and olefinic carbons. This may have been caused by a transient *trans*-nitroalkynyl species **12** which would might have arisen through a highly stereospecific 1,3-proton shift from (R_a)-allenenols **10**.[12b,18] Notably, an untransformed (*E*)-**3aD** was recovered with no deuterium incorporation at olefinic carbon (Scheme 2c). This indicates the absence of disfavored *syn*-nitroalkynyl species **11** which would have arisen upon 1,3-proton shift from (S_a)-allenenols **9**. Furthermore, we carried out a similar study with (*Z*)-**3a** and observed deuterium incorporation at olefinic carbon (*Z*)-**3aD** which indicated dynamic equilibrium between (*Z*)-**3a** and (R_a)-allenenols **10** under basic conditions (Scheme 2d).

We conducted two individual in situ NMR studies to understand the organocascade process more deeply. The first experiment reviewed the entire process and indicated (*E*)-**3a** to be a major isomer vs (*Z*)-**3a** with the consumption of nitro enyne **2a**; rapid growth of (*Z*)-**3a** was observed after DABCO addition at the expense of (*E*)-**3a**. In the second investigation, we performed the isomerization process separately with DABCO addition. Steady growth of (*Z*)-**3a** was observed progressively with the depletion of (*E*)-**3a** species.[13]

The formation of intermediates (*E*)-**3a** and (*Z*)-**3a** with or without the presence of DABCO was characterized computationally using density functional theory.[19] Experimentally, the addition of DABCO to the mixture of (*E*)-**3a** and (*Z*)-**3a** resulted in the depletion of (*E*)-**3a** as shown by NMR measurement. The barriers of deprotonation by DABCO was calculated in respect to the hydrogen bond complexes denoted as c*E*-**3a**··DABCO and c*Z*-**3a**··DABCO. The proton-transfer barrier to DABCO was predicted to be 18.21 and 14.41 kcal/mol for c*E*-**3a**··DABCO and c*Z*-**3a**··DABCO, respectively. The theoretical stability of the proton-transferred structures labeled as c*E*-**3a**$^-$··H$^+$DABCO and c*Z*-**3a**$^-$··H$^+$DABCO differed by 1.63 kcal/mol and favored the latter one. Subsequent detachment of H$^+$DABCO could further stabilize c*Z*-**3a**$^-$ by 2.06 kcal/mol over that of c*E*-**3a**$^-$. Substantial steric hindrance was anticipated and destabilized c*E*-**3a**$^-$ due to the repulsion between the phenyl group of allene moiety and the nitro group.

A tentative mechanism can be proposed according to our mechanistic controlled experiments and computational studies (Scheme 3). The bifunctional quinine-derived squaramide

Scheme 3. Plausible Mechanism for the Organocascade Process

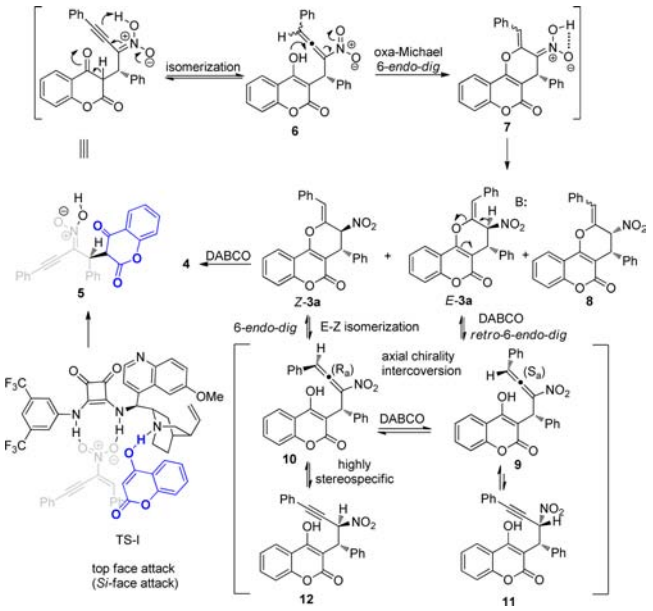

catalyst **I** delivers the 4-hydroxylcoumarin **1a** nucleophile to the *Si*-face of the 1,3-enyne through hydrogen-bonding interactions with both substrates (**1a** and **2a**) as shown in transition state TS-I. The alkynyl nitronate **5** undergoes a facile isomerization to elicit more labile nitroallene **6**.[12] Subsequently, a susceptible intramolecular oxa-Michael initiated 6-*endo*-*dig* cyclization evokes a complex *E*/*Z* mixture of *anti*- and *syn*-products **3** and **8**, respectively. The additional DBACO plays a vital role in transforming (*E*)-**3a** to (*Z*)-**3a**. The nucleophilic base additive performs a dual role, as it deprotonates the more acidic proton in (*E*)-**3a** through a *retro*-6-*endo*-*dig* cyclization to provide (S_a)-allenenol **9**, and it also it maintains a dynamic equilibrium between diastereomeric (S_a)- and (R_a)-allenenols (**9** and **10**).[20,5d] During the process, the intermediate (R_a)-allenenols **10** again undergo oxa-Michael initiated 6-*endo*-*dig* cyclization to afford predominantly (*Z*)-**3a**.

In conclusion, we developed an efficient process by using branched enynes and enols for the formation of annulated pyrans via central−axial−central chirality transformation.[21] The reaction proceeded smoothly through sequential conjugate addition, allene formation, intramolecular oxa-Michael 6-*endo*-*dig* cyclization, and DABCO-catalyzed olefin isomerization to give the desired products in high yields and excellent

DOI: 10.1021/acs.orglett.6b01265
Org. Lett. 2016, 18, 3098−3101

stereoselectivities. The study of α-alkynyl-substituted nitroolefins in organocatalytic reactions is currently underway.

■ ASSOCIATED CONTENT

Supporting Information

The Supporting Information is available free of charge on the ACS Publications website at DOI: 10.1021/acs.orglett.6b01265.

Experimental procedures, characterizations, NMR spectra, X-ray data, and computational details (PDF)

■ AUTHOR INFORMATION

Corresponding Authors

* E-mail: mktsai@ntnu.edu.tw.
* E-mail: kchen@ntnu.edu.tw.

Notes

The authors declare no competing financial interest.

■ ACKNOWLEDGMENTS

This study was supported by the Ministry of Science and Technology of Taiwan (MOST 102-2113-M-003-005-MY3 and 103-2113-M-003-005-MY2). We are grateful to the National Center for High-Performance Computing of Taiwan for providing computer time and facilities.

■ REFERENCES

(1) Genet, J.-P.; Toullec, P. Y.; Michelet, V. *Modern Alkyne Chemistry: Catalytic and Atom-Economic Transformations*; Trost, B. M., Li, C.-J., Eds.; Wiley−VCH, 2015; Chapter 3, p 27.

(2) (a) Belot, S.; Vogt, K. A.; Besnard, C.; Krause, N.; Alexakis, A. *Angew. Chem., Int. Ed.* **2009**, *48*, 8923. (b) Belot, S.; Quintard, A.; Krause, N.; Alexakis, A. *Adv. Synth. Catal.* **2010**, *352*, 667. (c) Li, X.; Li, X.; Peng, V.; Shao, Z. *Adv. Synth. Catal.* **2012**, *354*, 2873. (d) Cao, Z.-Y.; Zhao, Y.-L.; Zhou, J. *Chem. Commun.* **2016**, *52*, 2537.

(3) (a) Hack, D.; Chauhan, P.; Deckers, K.; Mizutani, Y.; Raabe, G.; Enders, D. *Chem. Commun.* **2015**, *51*, 2266. (b) Kaya, U.; Chauhan, P.; Hack, D.; Deckers, K.; Puttreddy, R.; Rissanen, K.; Enders, D. *Chem. Commun.* **2016**, *52*, 1669. (c) Hack, D.; Chauhan, P.; Deckers, K.; Hermann, G. N.; Mertens, L.; Raabe, G.; Enders, D. *Org. Lett.* **2014**, *16*, 5188. (d) Hack, D.; Dürr, A. B.; Deckers, K.; Chauhan, P.; Seling, N.; Rübenach, L.; Mertens, L.; Raabe, G.; Schoenebeck, F.; Enders, D. *Angew. Chem., Int. Ed.* **2016**, *55*, 1797.

(4) For reviews on combining organocatalysis and metal-mediated catalysis, see: (a) Du, Z.; Shao, Z. *Chem. Soc. Rev.* **2013**, *42*, 1337. (b) Allen, A. E.; MacMillan, D. W. C. *Chem. Sci.* **2012**, *3*, 633. (c) Chen, D.-F.; Han, Z.-Y.; Zhou, X.-L.; Gong, L.-Z. *Acc. Chem. Res.* **2014**, *47*, 2365.

(5) For selected metal catalysed reactions, see: (a) Han, J. W.; Tokunaga, N.; Hayashi, T. *J. Am. Chem. Soc.* **2001**, *123*, 12915. (b) Nishimura, T.; Makino, H.; Nagaosa, M.; Hayashi, T. *J. Am. Chem. Soc.* **2010**, *132*, 12865. (c) Wang, M.; Liu, Z.-L.; Zhang, X.; Tian, P.-P.; Xu, Y.-H.; Loh, T.-P. *J. Am. Chem. Soc.* **2015**, *137*, 14830. (d) Yao, Q.; Liao, Y.; Lin, L.; Lin, X.; Ji, J.; Liu, X.; Feng, X. *Angew. Chem., Int. Ed.* **2016**, *55*, 1859. For organocatalytic methods, see: (e) Zhang, W.; Zheng, S.; Liu, N.; Werness, J. B.; Guzei, L. A.; Tang, W. *J. Am. Chem. Soc.* **2010**, *132*, 3664. (f) Qian, H.; Yu, X.; Zhang, J.; Sun, J. *J. Am. Chem. Soc.* **2013**, *135*, 18020.

(6) (a) Neff, R. K.; Frantz, D. E. *Tetrahedron* **2015**, *71*, 7. (b) Campolo, D.; Gastaldi, S.; Roussel, C.; Bertrand, M. P.; Nechab, M. *Chem. Soc. Rev.* **2013**, *42*, 8434.

(7) Verrier, C.; Melchiorre, P. *Chem. Sci.* **2015**, *6*, 4242.

(8) For selected references, see: (a) Yu, X.; Ren, H.; Xiao, Y.; Zhang, J. *Chem. - Eur. J.* **2008**, *14*, 8481. (b) Xiao, Y.; Zhang, J. *Chem. Commun.* **2009**, 3594. (c) Yu, X.; Du, B.; Wang, K.; Zhang, J. *Org. Lett.* **2010**, *12*, 1876. (d) Yu, X.; Zhou, G.; Zhang, J. *Chem. Commun.* **2012**, *48*, 4002.

(9) Through isomerization of 3-butynoates to allenoates, see: (a) Sampath, M.; Loh, T.-P. *Chem. Sci.* **2010**, *1*, 739. (b) Liu, H.; Feng, W.; Kee, C. W.; Leow, D.; Loh, W.-T.; Tan, C.-H. *Adv. Synth. Catal.* **2010**, *352*, 3373.

(10) For selected works from this group, see: (a) Reddy, R. J.; Chen, K. *Org. Lett.* **2011**, *13*, 1458. (b) Roy, S.; Chen, K. *Org. Lett.* **2012**, *14*, 2496. (c) Roy, S.; Chen, K.-F.; Gurubrahamam, R.; Chen, K. *J. Org. Chem.* **2014**, *79*, 8955. (d) Gurubrahamam, R.; Cheng, Y.-S.; Chen, K. *Org. Lett.* **2015**, *17*, 430.

(11) (a) Ganesh, M.; Namboothiri, I. N. N. *Tetrahedron* **2007**, *63*, 11973. (b) Bharathiraja, G.; Sakthivel, S.; Sengoden, M.; Punniyamurthy, T. *Org. Lett.* **2013**, *15*, 4996.

(12) For isomerization of 3-alkynoates to allenoates, see: (a) Liu, H.; Leow, D.; Huang, K.-W.; Tan, C.-H. *J. Am. Chem. Soc.* **2009**, *131*, 7212. (b) Inokuma, T.; Furukawa, M.; Suzuki, Y.; Kimachi, T.; Kobayashi, Y.; Takemoto, Y. *ChemCatChem* **2012**, *4*, 983.

(13) See the Supporting Information.

(14) (a) Kshirsagar, U. A.; Parnes, R.; Goldshtein, H.; Ofir, R.; Zarivach, R.; Pappo, D. *Chem. - Eur. J.* **2013**, *19*, 13575. (b) Morito, K.; Aomori, T.; Hirose, T.; Kinjo, J.; Hasegawa, J.; Ogawa, S.; Inoue, S.; Muramatsu, M.; Masamune, Y. *Biol. Pharm. Bull.* **2002**, *25*, 48.

(15) Hua, D. H.; Huang, X.; Tamura, M.; Chen, Y.; Woltkamp, M.; Jin, L.-W.; Perchellet, E. M.; Perchellet, J.-P.; Chiang, P. K.; Namatame, I.; Tomoda, H. *Tetrahedron* **2003**, *59*, 4795.

(16) Detailed X-ray crystallographic data for *E*-**3a** [CCDC 1465297] are available from the Cambridge Crystallographic Data Centre, Cambridge, CB2 1EZ, UK.

(17) Wolf, F. F.; Klare, H.; Goldfuss, B. *J. Org. Chem.* **2016**, *81*, 1762.

(18) (a) Dabrowski, J. A.; Haeffner, F.; Hoveyda, A. H. *Angew. Chem., Int. Ed.* **2013**, *52*, 7694. (b) Zhang, W.; Ready, J. M. *ChemCatChem* **2013**, *5*, 3497.

(19) Two minimum structures were identified computationally for intermediate **5** (labeled as c**5a** and c**5b**, with c denoting the computational optimized structure for the rest of discussion). The structure of c**5a** was predicted to be 3.74 kcal/mol lower than that of c**5b**, and such relative energetics favored the subsequent formation of intermediates *E*-**3a** and *Z*-**3a** through an oxa-Michael 6-*endo*-*dig* process. The c**5b** structure could be transformed into two minor isomers of intermediate **8** denoted as c*E*-**8** and c*Z*-**8**. The relative free energy of these four isomers (c**5a**, c**5b**, c*E*-**8**, and c*Z*-**8**) was predicted as 0.00, 0.29, 9.28, and 5.62, respectively. The theoretical prediction was in good agreement with the experimental data for the formation of *E*-**3a** over *Z*-**3a** (see the Supporting Information for details).

(20) For DABCO-catalyzed cycloaddition of allenoates, see: (a) Chen, X.-Y.; Wen, M.-W.; Ye, S.; Wang, Z.-X. *Org. Lett.* **2011**, *13*, 1138.

(21) During the preparation of this manuscript, a DABCO-catalyzed domino process for the synthesis of racemic annulated (*Z*)-2-methylene pyrans was reported: Biswas, S.; Dagar, A.; Mobin, S. M.; Samanta, S. *Org. Biomol. Chem.* **2016**, *14*, 1940.

DOI: 10.1021/acs.orglett.6b01265
Org. Lett. 2016, 18, 3098−3101